Abstract

High inorganic phosphate may facilitate lung tumorigenesis at an early stage in K-ras^{LA1} mice

(Supervisor: Myung-Haing Cho, D.V.M., Ph.D.)

Somin Lee, M.S.

Interdisciplinary Program in Tumor Biology
College of Medicine
Graduate School of Seoul National University

Inorganic phosphate (Pi) is necessary for all living organisms because it affects the development of organs such as the bones, muscles, brains, and lungs by controlling several pivotal genes and regulating signal transduction. The aim of this study was to utilize a high phosphate diet (HPD) to determine, the concentration effects Pi-mediated signaling at different time intervals, in an in vivo system. Experiments were performed with K-rasLA1 lung cancer model mice. Mice were fed a normal diet (ND) containing 0.3% Pi and a high phosphate diet (HPD) containing 1% Pi for 1, 2 and 4 months. At the end of the experiment, all mice were sacrificed and were subjected to ICP-MS/OES, LA-ICP-MS analyses, Western blot, histopathological examination, immunohistochemistry (IHC), and immunofluorescence (IF) labeling. Results indicated that HPD accelerated tumorigenesis, and adenoma and adenocarcinoma incidence and tumor size increased significantly. However, at 4 months into the HPD using the K-ras LA1 lung cancer model, we observed suspended proliferation, massive ion level changes in the liver and lungs, energy generation via the tri-carboxylic acid (TCA) cycle in the liver, increased autophagy, and decreased angiogenesis and apoptosis. Taken together, these results indicate that HPD facilitates lung cancer promotion at an early stage of cancer development but after 4 months of HPD, tumorigenesis appears to slow down due to metabolic adaptation resulting

in quiescence, which can cause severe cancer promotion in later stages. Therefore, carefully regulated Pi consumption might a critical role in lung cancer prevention.

Keywords: high phosphate diet; inorganic phosphate (Pi); lung cancer; autophagy; protein translation; apoptosis; tumorigenesis.

Student number: 2012-21771

TABLE OF CONTENTS

ABSTRACT.....i

TABLE OF CONTENTS.....iii

LIST OF TABLES.....iv

LIST OF FIGURES.....v

LIST OF ABBREVIATIONS.....vi

Introduction.....1

Materials and Methods.....4

Results.....11

Discussion.....31

References.....38

Abstract in Korean.....43

LIST OF TABLES

Table 1. Diet composition of modified AIN-93G purified rodent diet …….....5

Table 2. ICP-MS and ICP-OES operational conditions……9

Table 3. Amount of daily food intake and inorganic phosphate and average of weight change of K-ras^{LA} mice in 1, 2, and 4 month of ND and PHD…….....12

Table 4. Summary of tumor incidence in the lungs of K-ras^{LA1} mice ……14

Table 5. Ion level changes in the 1-, 2-, and 4-month ND and HPD livers and lungs of K-ras^{LA1} mice …….....15

LIST OF FIGURES

Figure 1. HPD induced different tumorigenesis rates in the lungs of K-ras^{LA1} mice at different time points ……..……14

Figure 2. LA-ICP-MS analysis ……..16

Figure 3. Western blot analyses of p-acetyl CoA, acetyl CoA, SDHA (complex II), cytochrome *c* (complex III), COX IV (complex IV), and rieske (Fe-S complex) proteins in the livers of K-ras^{LA1} mice ……...19

Figure 4. Western blot analysis of autophagy related proteins in the lungs of K-ras^{LA1} mice and immunofluorescence staining of LC3 in tissue sections ……..…..22

Figure 5. Analysis of protein translation in the lungs of K-ras^{LA} mice …….24

Figure 6. Analysis of proliferation, angiogenesis, and epithelial-mesenchymal transition (EMT) in the lungs of K-ras^{LA} mice …….....28

Figure 7. Western blot analysis of the mitochondrion-mediated apoptosis-related proteins BAD, BAX, and cytochrome *c*, in the lungs of K-ras^{LA1} mice 30

LIST OF ABBREVIATION

Pi	Inorganic phosphate
HPD	High phosphate diet
ATP	Adenosine triphosphate
AIN	American Institute of Nutrition
IHC	Immunohistochemistry
IF	Immunofluorescence
PBS	Phosphate-buffered saline
LA-ICP-MS	Laser ablation-inductively coupled plasma-mass spectrometry
ICP-MS	Inductively coupled plasma mass spectrometry
ICP-OES	Inductively coupled plasma- optical emission spectrometer
H&E	Hematoxylin and eosin
NAD	Nicotinamide adenine dinucleotide
Q	Ubiquinone
GDP	Guanosine diphosphate
GTP	Triphosphate
LC3	1A/1B-light chain 3
ND	Normal diet
70S6K	70kDa ribosome protein S5 kinase
EMT	Epithelial-mesenchymal transition
PCNA	Proliferating cell nuclear antigen
NPT2b	Sodium-dependent phosphate co-transporter 2b
BMR	Basal metabolic rate
SDHA	Succinate dehydrogenase complex, subunit A
NSCLC	Non-small cell lung cancer
4E-BP-1	Eukaryotic initiation factor 4E binding protein 1
MOMP	Mitochondrial outer membrane permeabilization

INTRODUCTION

Inorganic phosphate (Pi) is an essential component required by all living organisms. Pi plays a role in mineral metabolism, diverse cellular functions involving intermediary metabolism, and energy-transfer mechanisms. It is fundamental for producing energy from membrane phospholipids and nucleotides as well as regulating phosphorylated intermediates in cellular signaling (Takeda et al., 2004). Access to sufficient Pi can be achieved through food intake or naturally. Currently, we are observing an increase in human Pi consumption related to increases in Pi availability in foods (Sheard et al., 1999). Various statistical data on food consumption indicate that Pi intake increased by approximately 17% in the decade prior to 1993, and the use of Pi in food additives has also continued to increase (Calvo et al., 1993).

It has been reported that ions in the body play a crucial role in regulating bio-metabolism. Our data revealed that a high phosphate diet (HPD) triggers ion induction and alters the levels of related ions *in vivo.* Ions such as Fe2+ or Ca2+ are crucial to metabolism. Intriguingly, the data that we acquired using LA-ICP-MS indicated that high Pi increased the levels of sulfur and iron ions, which present a sub-complex of cellular metabolism in the liver. Although we did not investigate in detail which signals can trigger ion extraction in the present study, our research suggest the possibility that these functions may be regulated by complexes that control adenosine triphosphate (ATP) synthesis.

Maintaining homeostasis is crucial for the survival of multicellular organisms, which

in turn depends on the ability of cells to sense and respond to intracellular and extracellular signals. Cells are thus able to maintain a balance between synthesis, degradation and recycling of different cellular components at a physiological level. Here, the concept of autophagy regulation is emphasized. Autophagy plays an essential role in promoting the cellular-survival mechanism under stress conditions (e.g., transient nutrient starvation and growth factor withdrawal) which forces a return to the homeostatic state (Atala et al., 2011). In low metabolic states, such as during a decrease in glucose uptake and glycolysis, the rate of protein translation is reduced and autophagy is activated in order to provide nutrients for survival. This quiescent state is a result of metabolic adaptation. In this study, we observed that low metabolic states from excessive Pi intake, over a certain period time, led to a counterbalance between proliferation of cancer cells through regulation of autophagy, and protein translation. However, adaptation to the continuous stressed-condition resulted in increasingly aggressive cancer cell development via mitochondrial-mediated apoptotic cell death pathways. Apoptosis is well-known to be involved in crucial cellular procedures related to the turnover of subcellular organelles and proteins (Nikoletopoulou et al., 2013).

In a previous study, Chang et al., 2006 reported that Pi works as a stimulus capable of increasing or decreasing the expression of a number of pivotal genes such as those involved in the regulation of transcription, signal transduction, and cell cycling. Additionally, Jin et al. 2009 indicated that a HPD promotes lung tumorigenesis related to altered Akt-signaling in 4-week-old K-ras^{LA1} lung cancer mouse model.

Appropriate regulation of Pi intake is crucial and is considered a key factor in maintaining health (Jin et al., 2009), (Chang et al., 2006). However, to date no definitive mechanistic studies have evaluated lung homeostatic maintenance during longer periods of high phosphate intake related to metabolic adaptation and cancer cell development. In this study, we report effects made to elucidate the effects of high Pi intake over different time periods, and the effects of HPD on lung cancer progression in K-ras^{LA1} mice.

MATERIALS AND METHODS

Animal experiment and its diet

Experiments were conducted on 5-week-old male K-*ras*^{LA1} mice, obtained from the Human Cancer Consortium – National Cancer Institute (Frederick, MD, USA). The animals were maintained in a laboratory facility with standard temperature of 23±2°C and relative humidity of 50±10% under a 12-hour light/dark cycle. All methods used this study were approved by the Animal Care and Use Committee at Seoul National University (SNU-120904-3-2). The 48 K-*ras*^{LA1} mice are randomly allocated to 6 groups (6 mice/ group); half of groups (1,2, and 4 months each) had an AIN93-based diet containing 0.3% Pi (normal phosphate diet) and half of groups (1,2, and 4 months each) had a same diet fortified with 1.0% Pi (high phosphate diet). All diets were prepared according to the guidelines of the American Institute of Nutrition (AIN) by Reeves and colleagues (Reeves et al., 1993). Body weight, amount of consumption of pallet, water was measured once per week. After 1, 2, and 4 month period of diet, mice were all sacrificed. All animals were anesthetized with 15mg/kg of Zoletil (Laboratoires Virbac, Carros, France) and 3mg/kg of xylazine (Laboratoires Calier, Barcelona, Spain), and perfusion were carried out. During the autopsy procedure, brain, thymus, heart, lung, liver, spleen, kidney, testis were taken out. Especially, lung was carefully taken out, and the tumor lesions on the entire lung surfaces were counted and lesion diameter was measured with the digital calipers under microscope as described by Singh et al.

Table 1. Diet composition of modified AIN-93G purified rodent diet

Ingredient	Normal Diet (0.3% Pi)	High Phosphate Diet (1%Pi)
Casein, g	200	200
L-cystine, g	3	3
Corn starch, g	397.486	397.486
Maltodextrin, g	132	132
Sucrose, g	100	100
Soybean oil, g	70	70
Cellulose (fiber), g	53.3	36.1
94047VM, AIN-93-VX, g	10	10
Choline bitartrate, g	2.5	2.5
t-Butylhydroquinone (antioxidant), g	0.014	0.014
AIN-93 Minearal mixture (excluding Ca, P), g	13.4	13.4
Calcium carbonate ($CaCO_3$), g	0	0
Calcium phosphate monobasic, g	3	31.5
Sodium phosphate monobasic, g	4	4

Histopathological examination, immunohistochemistry (IHC), and immunofluorescence (IF) labeling

The tissues were fixed in 10% buffered formalin, paraffin processed and sectioned at 5 μm on charged slide glasses (Fisher Scientific, Pittsburgh, PA, USA). For histopathologic analysis, tissue were de-paraffinized in xylene and rehydrated through alcohol gradients and then stained with hematoxylin and eosin (Sigma-Adrich, St Louis, MO, USA). For IHC, The tissue sections were de-paraffinized in xylene and rehydrated through alcohol gradients, then washed and incubated in 3% hydrogen peroxide (AppliChem, Darmstadt, Germany) for 30 min to quench endogenous peroxidase activity. After washing in phosphate-buffered saline (PBS), the tissue sections were incubated with 3% bovine serum albumin in TTBS for 1 hr at room temperature to block the unspecific binding sites. Primary antibody was applied to the tissue sections overnight at 4°C. The following day, the tissue sections were washed and incubated with secondary HRP-conjugated antibodies (1:50) for 1 hr at room temperature. After washing, tissue sections were counterstained with Mayer′s Hematoxylin (DAKO, Carpinteria, CA) and washed with xylene. Cover slips were mounted using Permount (Fisher), and the slides were reviewed using a light microscope (Carl Zeiss, Thornwood, NY). For immunofluorescence staining, the nuclear staining was carried out with 1ug/mL DAPI after blocking and washed out 3 times with PBS. LC3 primary antibody diluted 1:400 were applied overnight at 4°C. After rinsing, slides were incubated with fluorescein isothioncyanate-conjugated secondary antibody. Coverslips were mounted using DAKO cytomation Faramount aqueous mounting solution on

glass slides. Staining intensity was assessed by counting the number of positive cells in randomly selected fields viewed with appropriate magnification using In Studio version 3.01 (Pixera, San Jose, CA, USA).

Western blot analysis

The total protein concentration in the homogenized lung samples was determined using the Bio-Rad Protein Assay reagent (Bio-Rad, Hercules, CA, USA). Western blotting was performed following a previously described procedure. Antibody of p-Acetyl CoA (#3661), Acetyl CoA (#3676), LC3 (#2275), ATG5 (#2630), and p-Akt Thr308(2965) antibodies were purchased from Cell Signaling. SDHA (ab14715) and COX IV (ab33985) antibodies were purchased from Abcam. Cytochrome c (A-8), Rieske (A-5), Bad (C-7), Bax (B-9), Bcl-2 (C-2), FGF-2 (147), PCNA (PC10), N-cadherin and Actin (I-19) antibodies were purchased from Santa Cruz Biotechnology (Santa Cruz, CA, USA). GAPDH (LF-PA0212) antibody was purchased from Abfrontier. The bands were detected using the LAS-3000 luminescent image analyzer (Fujifilm, Tokyo, Japan). The Western blot bands analysis was quantified using the Multi Gauge version 2.02 software (Fujifilm).

Changes of trance elements in tissue

For laser ablation-inductively coupled plasma-mass spectrometry (LA-ICP-MS), we used a New Wave Research UP-213 laser ablation system equipped with a Nd:YAG

laser emitting a nanosecond laser pulse in the fifth harmonic with a wavelength of 213 nm. The laser was connected to an Agilent Technologies 7500cs ICP-MS by Tygon tubing. Details of our analytical methods have been published previously (Hare et al., 2010). In brief, the laser beam was rastered along the sample surface in a straight line. A laser spot size of 30 μm, laser scan speed of 60 μm s−1 and ICP-MS total integration time of 0.50 s produced data points that corresponded to a pixel size32 of approximately 900 μm2.

For ICP-MS, ICP-OES analysis, tissue samples were digested in sulfuric acid and hydrogen peroxide for elemental analysis. All chemical reagents were of analytical grade. Water (resistivity of 18.2MΩ) was de-ionized in a Milli-Q system (Millipore, Bedford, MA, USA). A 65% v/v nitric acid and 95-97% v/v sulfuric acid both from Samchun Chemical were used for the preparation of samples. Acid digestion occurred at 70°C for 24 hours followed by hydrogen peroxide (70°C) digestion overnight. Tissue samples were diluted with MO water to an acid concentration of 0.2%. The concentrations of elemental Mn, Fe, Cu, and Zn were quantified using inductively coupled plasma mass spectrometry (ICP-MS) and the concentration of elemental Na, Ca, S, P were measured using inductively coupled plasma- optical emission spectrometer (ICP-OES). The ICP-MS and ICP-OES operational conditions are described in table 2.

Table 2. ICP-MS and ICP-OES operational conditions.

Parameter	ICP-MS	ICP-OES
Model / Maker	7700 / Agilent, Japan	5300DV / PerkinElmer Optima
RF generator power, W	1550	1300
Argon gas flow rate		
Plasma, L/min	15	15
Carrier, L/min	0.8	0.5
Makeup, L/min	0.35	0.65
Collision gas (He), mL/min	4	1
Replicates	3	3
Isotopes monitored	Mn, Zn, Cu, Fe	Na, Ca, S, P

Statistical analyses

Statistical analyses were performed with a *student's* t *test* for experiments that consisted of *two groups* (Graphpad Software, San Diego, CA, USA) and data are presented as the Mean ± SEM. *P value < 0.05 was considered as significant and **P < 0.01, ***P < 0.001 were highly significant compared with the corresponding control values.

RESULTS

HPD for 1 and 2 months accelerates tumorigenesis in the lungs of K-ras^{LA1} mice.

To determine the potential effects of high Pi on pulmonary tumor growth, tumor lesions on the surface of the lungs in each group were carefully measured. Our results indicated that high levels of Pi consumption induced pulmonary cancer development over periods of 1, 2, and 4 months (Table 3). In HPD groups measured over 1 or 2 months, the number, size and volume of tumor nodules were significantly increased compared with those in the ND group; however, changes were insignificant in the 4-month HPD group (Figure 2B). Histopathological examination of the 4-month HPD group also clearly indicated a 2-fold increase in the number of carcinoma and adenocarcinoma incidents in 1- and 2-month HPD groups. The entire HPD group exhibited progression of adenocarcinoma and adenoma with dense populations of tumor cells in hematoxylin and eosin (H&E) staining. However, at 4 months for the HPD group, the incidence rate of adenocarcinomas and adenomas was alleviated, followed by the reemergence of near-normal structures of the lungs with a single lining of alveolar walls (Figure 2C). The overall tumor incidences are summarized in Table 4.

Table 3. Amount of daily food intake and inorganic phosphate and average of weight change of K-rasLA mice in 1, 2, and 4 month of ND and PHD. The results are shown as AV±SD. *P<0.05;**P<0.01; ***P<0.001

	1-month		2-month		4-month	
	ND	HPD	ND	HPD	ND	HPD
Daily Feed Intake (g/mouse)	2.45±0.62	2.88±2.41	2.85±1.37	3.01±3.23	3.21±2.49	3.56±3.29
Daily Consumption of Pi (mg/mouse)	17.15±0.61	102.24±1.45***	19.95±1.05	106.86±2.17***	22.47±0.84	126.38±0.85***
Average of Weight Changes(g)	5.34±1.72	5.36±2.98	10.14±2.36	10.79±2.98	12.72±1.08	12.38±1.70

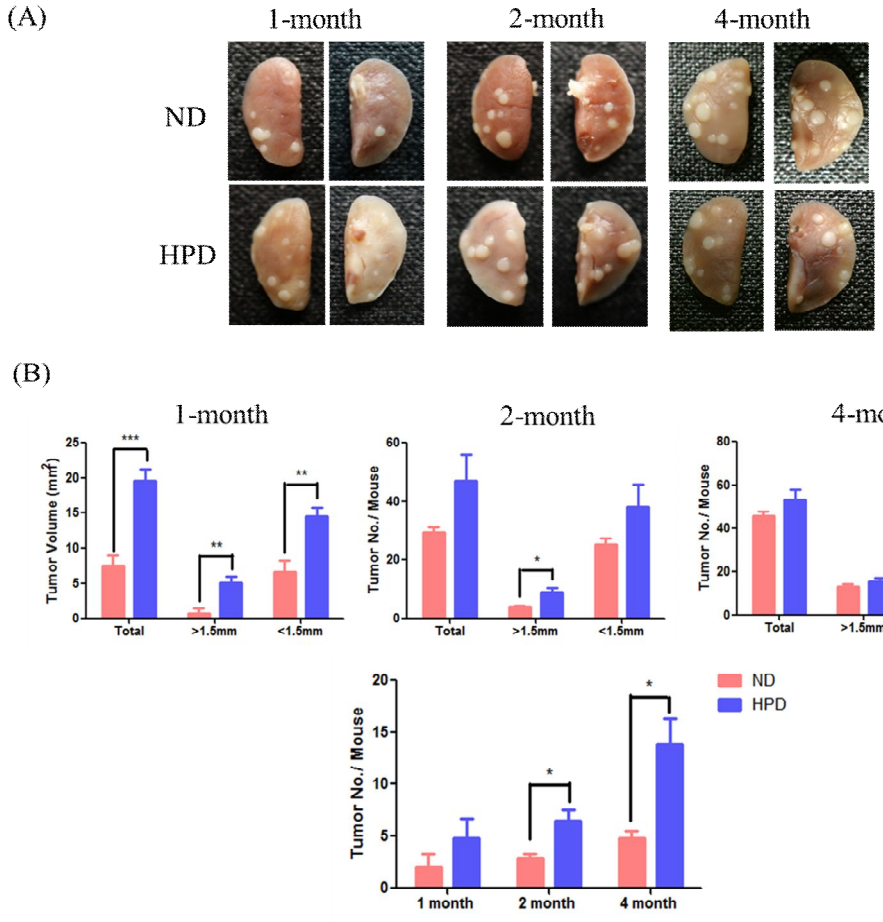
(A)
1-month
2-month
4-month
ND
HPD
(B)
1-month
2-month
4-month
Tumor Volume (mm³)
Tumor No./ Mouse
Total
>1.5mm
<1.5mm
ND
HPD
1 month
2 month
4 month
(C)
1-month
2-month
4-month
ND
HPD

Figure 1. HPD induced different tumorigenesis rates in the lungs of K-ras^{LA1} mice at different time points. (A) Murine lungs following dietary consumption of normal (0.3%) and high (1%) phosphate levels. (B) Total number of tumors and number of tumors with diameter >1.5 mm in ND and HPD mice. (C) H&E staining revealing the tumor expression aspect of ND and HPD.

Table 4. Summary of tumor incidence in the lungs of K-ras^{LA1} mice

ND (n=6)	Adenocarcinoma	Adenoma	HPD (n=6)	Adenocarcinoma	Adenoma
1-month	1	3	1-month	2	9
2-month	3	12	2-month	6	14
4-month	6	14	4-month	7	17

HPD induced ion level changes in the lungs of K-ras^{LA1} mice.

The liver is a crucial organ for digestion, and for regulation of most chemical levels in the blood. Blood leaving the stomach and intestines passes through the liver, which breaks down the component nutrients. Since this metabolic regulation in the liver occurs via ion level changes, we quantitatively analyzed various ion levels. Ion changes in between ND and HPD were measured and compared via ICP-MS, ICP-OES, and LA-ICP-MS, and results of these analyses revealed. In contrast to ND, massive ion level changes detected in HPD livers and lungs. The 4-month HPD livers exhibited higher levels of P, S, Na, Fe, Mn, Cu, and Zn than ND, while the 4-month HPD lungs exhibited decreased levels of Ca, Na, Fe, Cu, and Zn, but P or S (Figure 2 and Table 5). Insignificant ion levels were detected in the 1- and 2- month groups.

Table 5. Ion level changes in the 1-, 2-, and 4-month ND and HPD livers and lungs of K-ras^{LA1} mice

	1-month				2-month				4-month			
	Liver		Lung		Liver		Lung		Liver		Lung	
	ND	HPD	ND	HPD	ND	HPD	ND	HPD	ND	HPD	ND	HPD
P (ug/g)	3041.5	3334.8	2048.6	2146.4	3371.3	3570.6	2598.6	2724.7	2870.9	3380.7	2229.8	2396.2
S (ug/g)	2620.2	2908.5	ND	89.4	2735.2	3043.4	2.5	274.4	2330.2	9222.1	167.6	308.9*
Ca (ug/g)	22.9	47.1	22.5	ND	26.4	58.0	33.3	98.8	92.3	63.5	60.8	86.2
Na (ug/g)	587.9	679.3	2242.7	2046.6	645.7	544.8	4909.9	2452.6	587.9	722.4	2133.5	2111.0
Fe (pg/g)	86186.2	102044.0	29003.6	48475.1	113192.7	96882.5	63109.7	52227.8	71967.5	179979.0*	55675.8	53743.4
Mn (pg/g)	685.8	554.0	ND	ND	734.4	614.1	ND	ND	480.3	665.4*	ND	ND
Cu (pg/g)	6042.6	7328.3	2695.4	2195.7	6682.5	6734.2	43564.5	3413.9	3882.9	6586.7	4411.8	2340.3
Zn (pg/g)	25118.7	26758.8	11980.6	13108.0	28190.6	27771.9	14991.7	17246.1	27646.1	36710.3	44378.2	34992.3*

n = 6 in each group. Quantitative analysis of ion level changes measured by ICP-MS and ICP-OES. Results are presented as mean ± SD. *P < 0.05; **P < 0.01; ***P < 0.001

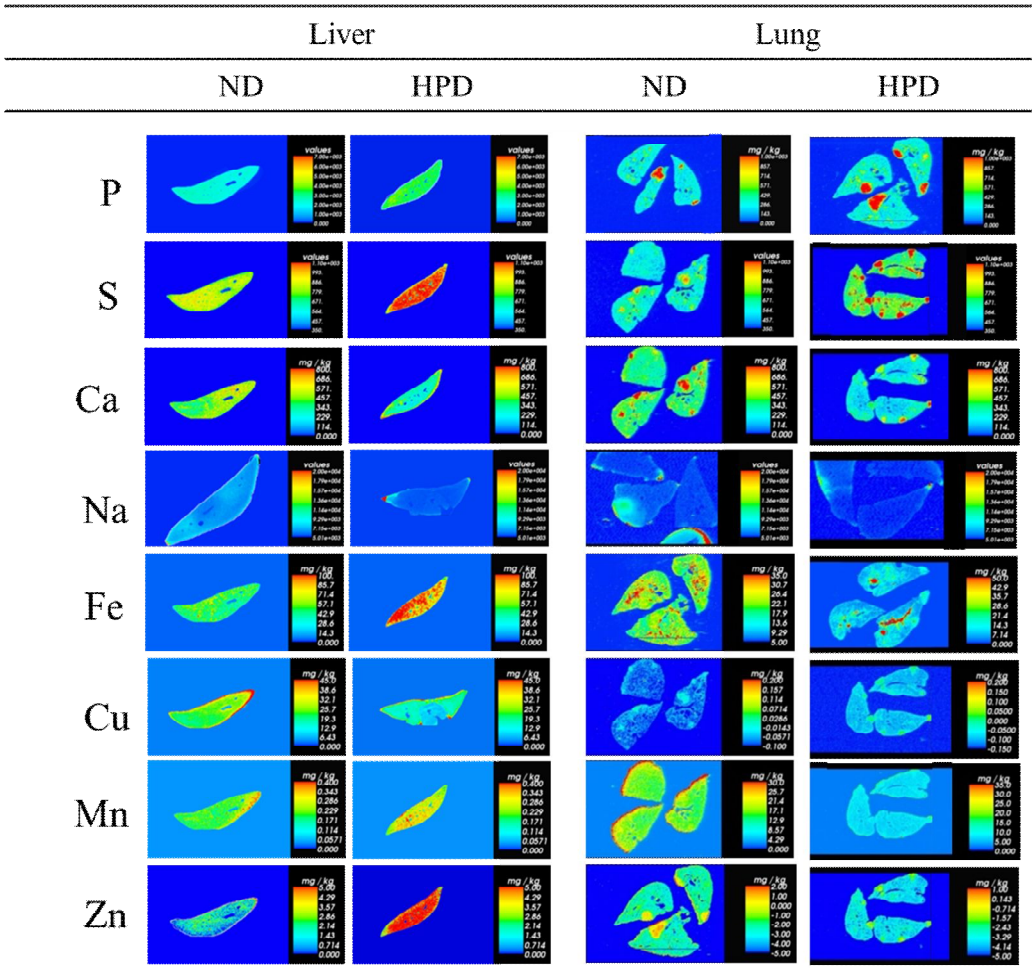

Figure 2. LA-ICP-MS analysis. Solution-ICP-MS/ICP-OES data represent the mean values for three trials.

HPD produced energy via the TCA cycle in the liver of K-ras^{LA1} mice.

The TCA cycle is a metabolic pathway that produces energy in living organisms, beginning with the transfer of a two-carbon acetyl group from acetyl-CoA to oxaloacetate. One complete turn of the cycle results in the following reactions: conversion of three equivalents of nicotinamide adenine dinucleotide (NAD+) into three equivalents of NADH; conversion of one equivalent of ubiquinone (Q) into one equivalent of QH2 related to the electron transport chain reaction; and conversion of one equivalent each of guanosine diphosphate (GDP) and triphosphate (GTP). Complexes I, II, III, and IV are essential proteins that play important roles in cellular respiration and ATP production (Tuquet et al., 2000),(Baymann et al., 2012), (Nomikos et al., 2004), (Patsiaoura et al., 2008), and (Rossi et al., 1968). In this study, we performed Western blotting analysis only using p-acetyl CoA, acetyl CoA, and complex II, III, and IV antibodies. As seen in Figure 3, the expression level of acetyl CoA in the HPD group liver was reduced, and was barely detectable even in the 4-month group bands. The levels of complexes II, III, and IV increased in the HPD liver group as indicated by the reaction of acetyl CoA and production of ATP in the activated TCA cycle. Cellular metabolism also mediated protein, function, and the Fe-S Rieske complex level was observed to increase in the HPD group. In conclusion, HPD was observed to trigger abnormal cellular metabolism and produce more ATP than ND.

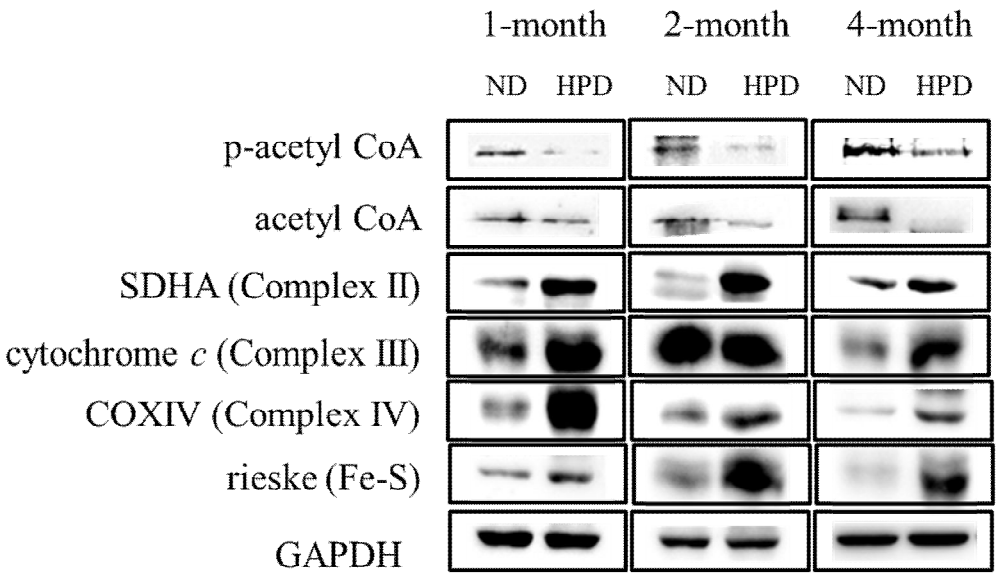
1-month
2-month
4-month
ND
HPD
ND
HPD
ND
HPD
p-acetyl CoA
acetyl CoA
SDHA (Complex II)
cytochrome c (Complex III)
COXIV (Complex IV)
rieske (Fe-S)
GAPDH

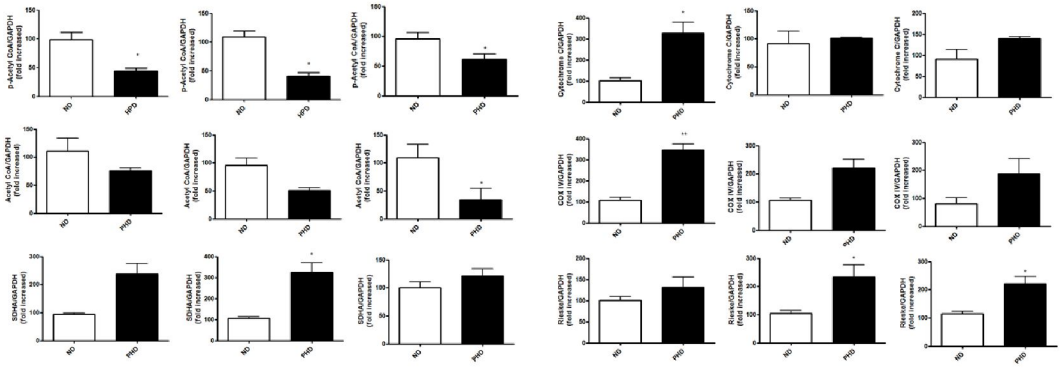

Figure 3. Western blot analyses of p-acetyl CoA, acetyl CoA, SDHA (complex II), cytochrome *c* (complex III), COX IV (complex IV), and rieske (Fe-S complex) proteins in the livers of K-ras^{LA1} mice. Five-week-old K-ras^{LA1} male mice were fed either a normal (ND) or high phosphate diet (HPD) for 4 months. Liver tissue homogenates were subjected to Western blot and densitometer analyses.

HPD increased autophagy in the lungs of K-ras^{LA1} mice.

Activation of autophagy was also considered as a means to examine the LC-3 protein level (Kuma et al., 2007). Microtubule-associated protein 1A/1B-light chain 3 (LC3) is a soluble protein distributed ubiquitously in mammalian tissues and cultured cells. Lysosomal turnover of the autophagosomal marker LC3-II reflects a starvation-induced cellular level of autophagy (15). Western blots were performed to confirm the activation of autophagy-related proteins. Results indicated an increase in ATG5 and LC3 levels 4-month lung lysates, but no significant differences in 1- and 2-month lung lysates (Figure 5A). IF was performed with parafin-sectioned slides representing each month's samples and images were taken of the tumor lesions. Few LC3 dots were observed in the 1- and 2- month samples (data not shown), while the 4-month HPD group exhibited four times as many flourescent dots as observed with the ND group. These results indicated that increasing the duration of Pi intake resulted in increased autophagic activity in the tumor lesion.

(A)

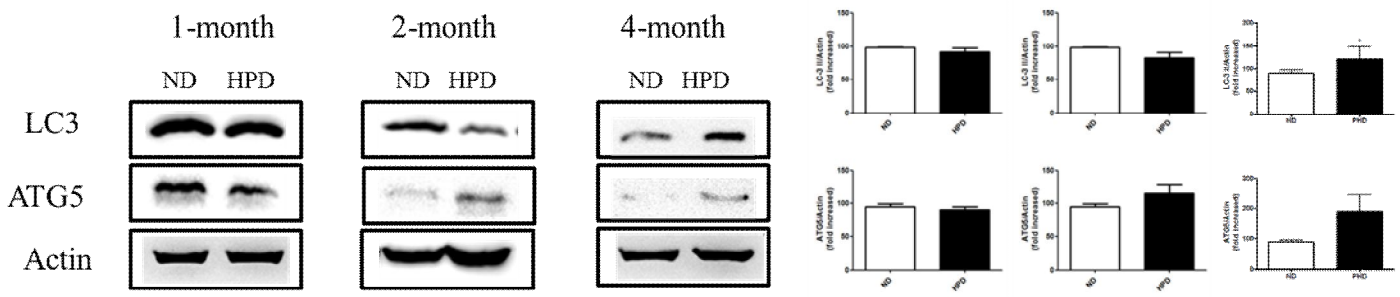
1-month
2-month
4-month
ND HPD
ND HPD
ND HPD
LC3
ATG5
Actin

(B)

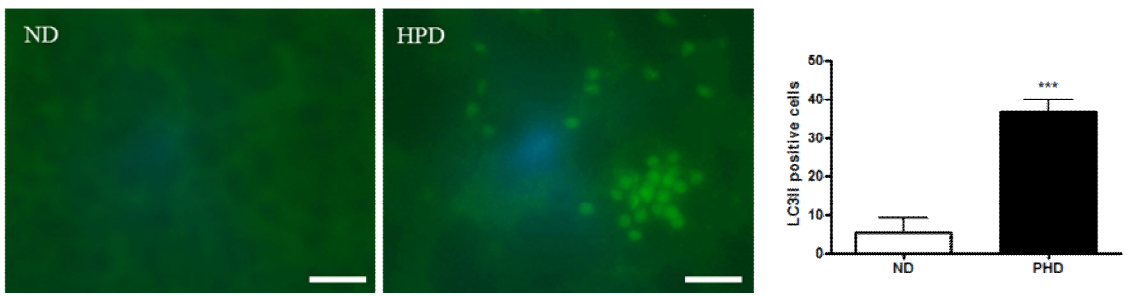
ND
HPD
LC3II positive cells
***
ND
PHD

Figure 4. (A)Western blot analysis of autophagy related proteins, LC3 and ATG5, in the lungs of K-ras^{LA1} mice. Five-week-old K-ras^{LA1} male mice were fed with ND and HPD for 1-, 2-, and 4-months. Lung tissue homogenates were subjected to Western blot analysis. (B) Immunofluorescence staining of LC3 in tissue sections. The green fluorescence intensity increased in lung lesions of the long-term HPD group. Magnification: x 200. Scale bar: 20 μm. The long-term HPD group displayed stronger green color than the ND group (control). Densitometic analysis of representative proteins.

Total protein translation level is increased in HPD at early stage of tumor development in K-ras^{LA1} mice.

The mTOR pathway controls cellular protein translation through regulation of p70S6K and 4E-BP1 phosphorylation, and protein translation is closely related with cell growth. In this study, we investigated changes in expressions of p-70kDa ribosome protein S5 kinase, (p70S6K) and eIF4E and 4E-BP1/2. Our results indicated that total protein translation levels increased in the 1- and 2- month HPD groups, but not in the 4-month HPD group.

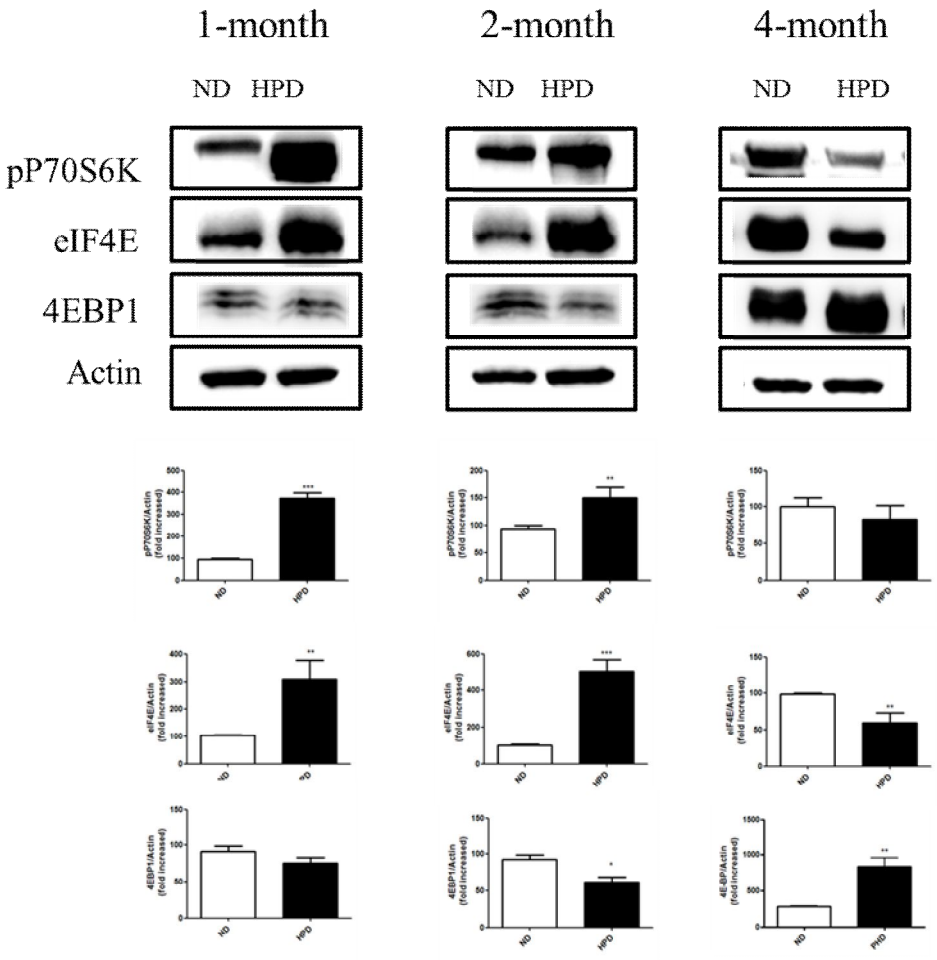

Figure 5. Analysis of protein translation in the lungs of K-ras^{LA} mice. (A) Western blot analysis of the protein translation-related proteins, P70S6K, eIF4E, p-4E-BP-1/2, and 4E-BP-1/2 in the lungs of K-ras^{LA1} mice. Lung tissue homogenates were subjected to Western blot analysis. Blots were probed with antibodies as indicated. Densitometric analysis of representative proteins.

Proliferation, angiogenesis, and epithelial-mesenchymal transition (EMT) are depressed in lungs of HPD group K-ras^{LA} mice

Proliferating cell nuclear antigen (PCNA) was selected as a marker, and a Western blot was performed to examine the correlation between tumor regression and cell proliferation. Angiogenesis (i.e., the sprouting of new blood vessels) plays a role in diverse pathologies including neoplastic, inflammatory, and degenerative conditions. To investigate the level of angiogenesis in 4-month HPD, we measured the expression levels of FGF-2 proteins by Western blot. As seen in Figure 7, the lungs for 1- and 2- month HPD groups exhibited increases in both markers compared with ND. Conversely, the 4-month HPD group exhibited decreased protein expression. These results demonstrated that tumor growth and progression was depressed in the 1- and 2-month groups, especially following high Pi intake. Data from IHC were consistent with the Western blot data, as more PCNA dots were observed in slides from the 1- and 2-month samples than in the 4-month samples (Figure 7B).

Strong expression of the EMT marker is correlated with the resistance of carcinoma epithelia cell lines to chemical drugs, as well as radiotherapy, by inhibiting apoptosis. Our results indicated that proliferation and angiogenesis expression were not significant in the 4-month lung lysates, expression of the EMT marker N-cadherin, continued to increase in the 4-month HPD group.

(A)

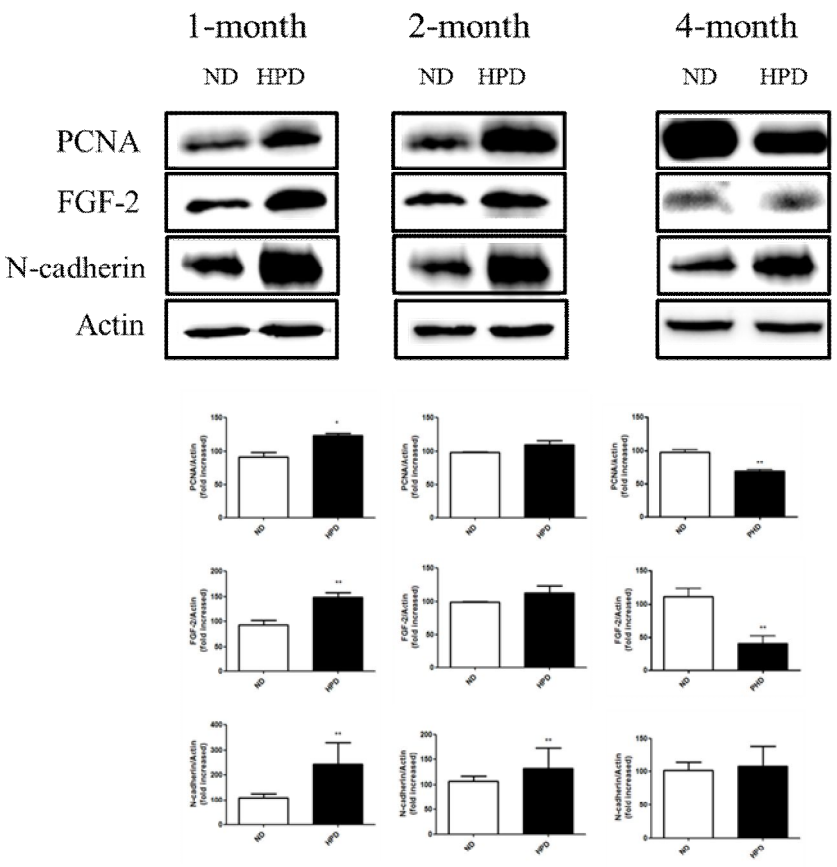
1-month
2-month
4-month
ND HPD
ND HPD
ND HPD
PCNA
FGF-2
N-cadherin
Actin
PCNA/Actin (fold increased)
FGF-2/Actin (fold increased)
N-cadherin/Actin (fold increased)
ND
HPD

(B)

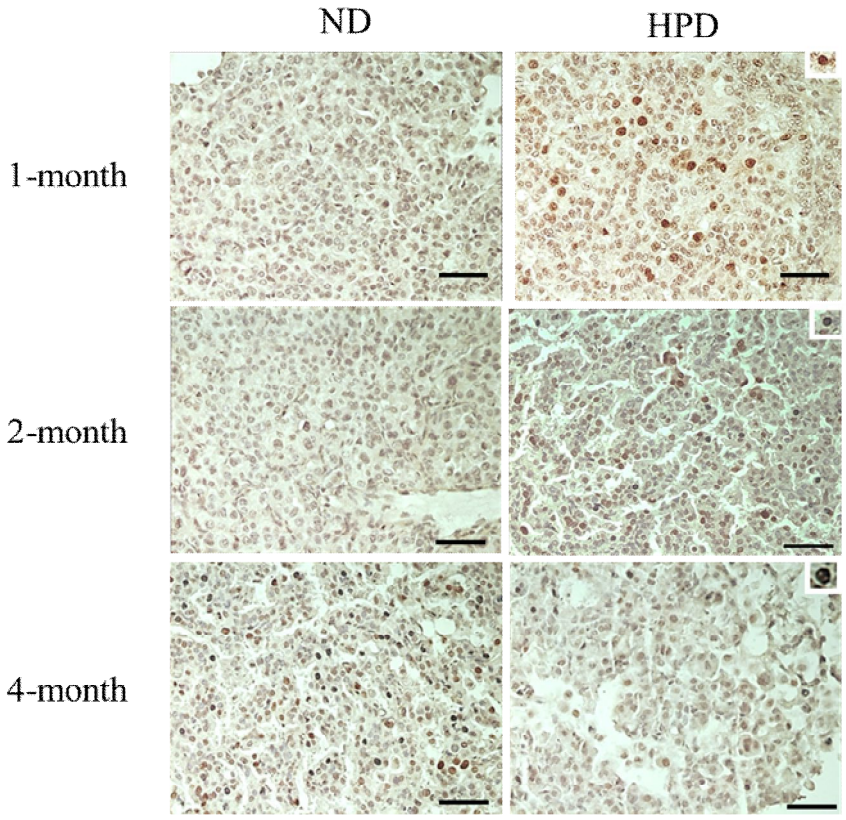

Figure 6. Analysis of proliferation, angiogenesis, and epithelial-mesenchymal transition (EMT) in the lungs of 1-, 2-, and 4-month ND and HPD K-ras^{LA} mice. (A) Western blot analysis of proliferation and angiogenesis related proteins, PCNA and FGF-2 in the lungs of K-ras^{LA1} mice. Lung tissue homogenates were subjected to Western blot analysis. Blots were probed with antibodies as indicated. (B) Immunohistochemistry of PCNA from the tumor region. PCNA positive cells are presented in the upper right corner of the control panel. Magnification: x 200. Scale bar: 20 μm.

HPD decreased mitochondrial mediated apoptosis in the lungs of K-ras^{LA1} mice.

Apoptotic figures are one of the hallmarks of cancers. Evasion of apoptosis may contribute to carcinogenesis, cancer proliferation, and resistance to therapy resistance. To analyze mitochondria-mediated apoptosis, we measured the protein expression levels of BAD, BAX, Bcl-2, and cytochrome *c* using western blotting. Our results indicated protein expression levels were reduced in the 1-, 2-, and 4-month HPD groups compared to the ND group. In conclusion, we determined that HPD mediation of apoptotic activity via mitochondria is inhibited.

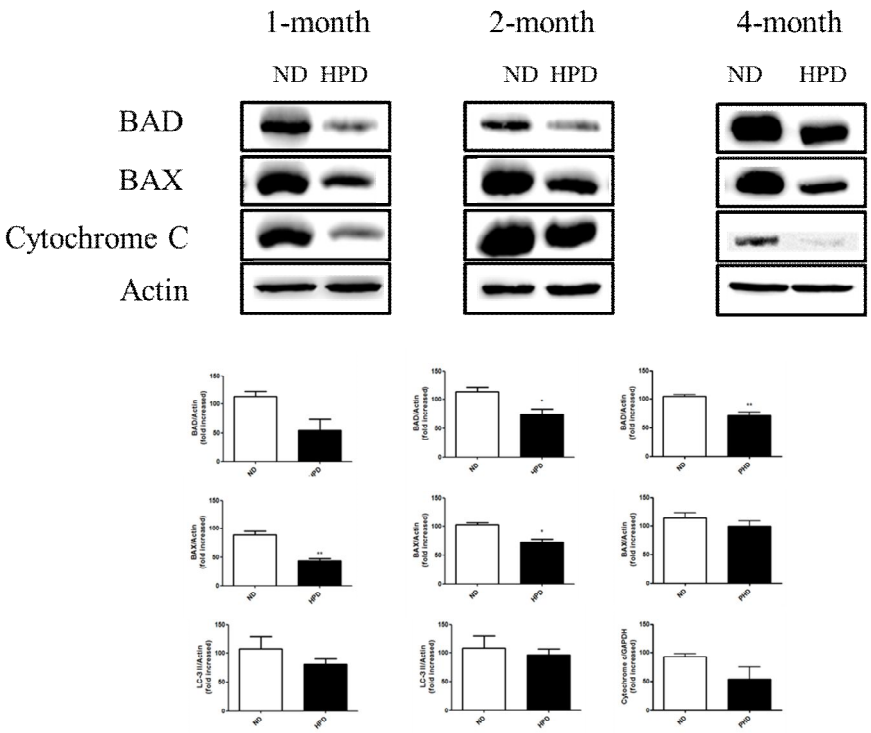

Figure 7. Western blot analysis of the mitochondrion-mediated apoptosis-related proteins BAD, BAX, and cytochrome *c*, in the lungs of K-ras^{LA1} mice. Five-week-old K-ras^{LA1} male mice were fed ND or HPD for 1-, 2-, and 4-months. Lung tissue homogenates were subjected to Western blot analysis. Blots were probed with antibodies as indicated.

DISCUSSION

Neoplastic growth is a cellular change involving an imbalance between cell proliferation, DNA repair, and cell death. Improper growth may involve either endogenous or exogenous chemical exposure. Beck et al reported that phosphate might be an important global signaling molecule capable of regulating the expression of a variety of genes in multiple cell types and multiple tissue types. Pi is present in fungus, bacteria, plant, and animal cells (Moreno-Torres et al., 2001). It plays a key role in diverse cellular functions involving mineral metabolism, intermediary metabolism, and energy-transfer. Furthemore, Pi is a vital component of membrane phospholipids, nucleotides that provide energy, RNA and DNA and is necessary for phosphorylated intermediates in cellular signaling (Takeda et al., 2012).

Recent studies have reported that regulation of sodium-dependent phosphate co-transporter 2b (NPT2b) plays an important role in regulating lung cancer growth. Moreover, NPT2b has also been found to be highly expressed in stage I and stage III human lung cancer tissues, but not in stage II. To investigate this seeming anomaly, we examined tumor development in K-ras^{LA1} mice at different time points.

Previous studies have reported that HPD correlates with tumorigenesis in 5-week-old lung cancer model mice following 1-month HPD treatment and enhanced cap-dependent translation and increased tumorigenesis through the Akt-signaling pathway in the brain, lung, and liver of mice. However, effects

associated with longer periods of HPD have not been reported, so the objective of this study was to elucidate the effects of 1-, 2-, and 4-month HPD on lung cancer using K-ras^{LA1} mice.

Mice in the experiment were fed a version of the AIN-93 diet (Dyets Inc., Bethlehem, PA), which lacked calcium and phosphorous (for Pi). We modified the composition of the original rodent pallets, according to the AIN-93G diet, by replacing the missing calcium and phosphorous (as sodium phosphate) to meet the ND (0.5% Ca, 0.3% P) and HPD (0.5% Ca, 1% P) condition.

As indicated in Table 2, daily consumption of Pi increased over time on this diet. Weights associated with mice in the 4-month HPD group decreased slightly compared with the 4-month ND group, which is consistent with reports that energy consumption associated with constant energy supplementation is expected to accelerate metabolism, leading to weight loss. Figure 2B, as large-scale ion level and phosphorus levels were observed in the 4-month HPD group. However we could not determine from these data whether a relationship exited between changes in the levels of trace elements and cancer development.

Quantitative analysis of the Fe-S Reiske complex using LA-ICP-MS indicated increases in Fe and S levels in the liver, and these increases were likely due to up-regulation of the cellular metabolism network. Additionally, no apparent ion increases were observed using Na as a negative control, but increases were observed following Pi uptake. Previous studies have indicated that increasing metal ion intake increased the likelihood of cancer development of the matter for cell proliferation controlling or anti-cancer agent controlling

like p53 (Stevens et al., 1994). For example, Ca^{2+}, which acts as a mitogen within the cytoplasm, is a versatile factor for controlling cell proliferation (Durham et al., 1982). Elevation of Fe^{3+} may trigger the risk of cancer occurrence, while high levels of Zn^{2+} induce loss of mitochondrial potential and degradation of Bcl-2 protein. Damage to Bcl-2 has been identified as a causal factor in a number of cancers, including melanoma, breast, prostate, chronic lymphocytic leukemia, and lung cancer (Untergasser et al., 2000). According to our data (Figure 2), it can be inferred that a long-term HPD induces the elevation of specific metal ions and gives rise to tumorigenesis.

In Figure 3, it can be seen that the basal metabolic rate (BMR) also increased in the HPD group as Pi activates the TCA cycle in the liver by rapidly consuming acetyl-CoA, resulting in the generation of more energy transferred to a part of body. Expression levels of electron transport chain system-related proteins such as Succinate dehydrogenase complex, subunit A (SDHA), cytochrome *c*, COX IV, and Rieske were observed to increase in HPD mice group. Furthermore, acetyl coenzyme A, the rate-limiting agent, was consumed for ATP generation. Therefore, according to our experimental data, HPD triggers cellular metabolism and produces more ATP than ND.

The role of autophagy in the promotion of tumor cell survival remains controversial, as activated autophagy can be detected under both hypoxic and starved conditions of the tumor microenvironment (Fimia et al., 2010). When tumors exhibit enhanced adaptations to respond to hypoxia, cancer cells display defined metabolic characteristics such as up-regulation of glycolysis,

and oxidative stress. This adaptation mechanism in autophagic activity promotes cancer cell dormancy. Once a tumor becomes quiescent, autophagic activity promotes adaptation to stress. LC3-II production represents an induction of autophagy, which is triggered by down-regulation of the the AKT and JNK and activation of the ERK1/2 pathway (Wei et al., 2008). In this study, we observed that LC3-II and ATG5 levels increased in the lungs from the 4-month HPD group (Figure 3), and these results are supported by recent studies indicating that activation of autophagy is correlated with adaptation of tumor growth.

Another recent study reported that approximately 90% of non-small cell lung cancer (NSCLC) cells were associated with activation of the mTOR-Akt pathway and that activation of this pathway promoted cell survival and resistance to therapy (Mamane et al., 2006). The p70kDa ribosome protein S6 kinase (p70S6K) regulates cellular protein translation via the mTOR pathway. Inactivation of p70S6K is known to suppress cell growth (Hsieh et al., 2010). Additionally, eukaryotic initiation factor 4E binding protein 1 (4E-BP-1) phosphorylation and protein translation are closely related to tumor promotion. A variety of malignances exhibit activated 4E-BP1 expression (Flynn et al., 1997). Translation initiation by binding to eIF4E occurs through interaction with 4E-BP1 and by inhibiting recruitment of the translation complex to mRNA. 4E-BP1 prevents translation by binding to eIF4E (Fujimura et al., 2012). Hyper-phosphorylation of 4E-BP1 releases it from eIF4E enabling assembly of the eIF4F complex, which permits translation to proceed (Yang et

al., 2007). Translation initiation is the rate-limiting step of protein synthesis. As eIF4E is the least abundant among the initiation factors and is considered to be the rate-limiting factor for cap-dependent translation initiation, changes in the levels of eIF4E profoundly affect the translation rates (Ducker et al., 2013). In the present study, we found expression level of pP70S6K and eIF4E is increased in 1 and 2 month HPD lung lysate that leads to rapid total protein translation occurrence compared to 4-month diet group. In conclusion, the early stage of tumor cell progression via HPD is accelerated by total protein translation.

Cell proliferation and angiogenesis are markers that predict the fate of tumorigenesis. Cancers have a tendency to grow quickly and may metastasize to other organs. Therefore, checkpoints that allow us to anticipate the prognosis of tumors would include PCNA for proliferation and FGF-2 and CD31 for angiogenesis in the tumor regions. Our results revealed increases in protein expression of PCNA and FGF-2 in 1- and 2-month HPD group lungs, while reduced protein expression levels observed with PCNA, and FGF-2 in the 4-month HPD group, were associated with cancer cell adaptation and autophagy in a hypoxic environment. Its growth seems to be slowed down; however, this is not actually the case. The EMT protein is typically correlated with tumor aggressiveness; however, in this study, we observed that proliferation and angiogenesis expression was not significant in the 4-month HPD lung lysates, while expression of the EMT marker, N-cadherin, continued to in the 4-month HPD group. We therefore assume that tumor

growth adapted to the excessive supplementation with Pi, which prolonged the low energy metabolic state, leading to quiescence of tumor cell growth. During metabolic adaptation, cancer cells can potentially develop drug resistance and aggressive cancer growth capabilities as a result of long-term exposure. Moreover, high levels of N-cadherin were detected in all HPD groups, suggesting that HPD leads to aggressive cancer growth.

Apoptosis also provided evidence to indicate that HPD results in more aggressive cancer cell growth. Apoptosis, or programmed cell death, is a physiological process that provides an effective, non-inflammatory way to remove redundant or damaged cells from tissues, thereby stabilizing tissue homeostasis. One of the caspase activation pathways is the intrinsic or mitochondrial pathway. The intrinsic pathway is triggered upon disruption of mitochondria, for example, as a result of DNA damage, resulting in the release of cytochrome *c* into the cytoplasm. BAX then translocates from the cytoplasm to the mitochondrial membrane where it forms pore-like structures resulting in mitochondrial outer membrane permeabilization (MOMP), which enables the subsequent release of cytochrome *c*. The result of this study indicated that the expression levels of BAD, BAX, BCL-2, and cytochrome *c* decreased in the HPD group (Figure 7), thereby suggesting that HPD induces inhibition of apoptosis in lung cancer, resulting in increased cancer cell aggressiveness.

In conclusion, these results demonstrated that HPD accelerates cancer cell growth during the early stage (i.e. the first 2 months) and that long term HPD

leads to aggressive pulmonary cancer cell growth. Therefore, regulated Pi consumption might be critical for lung cancer prevention.

REFERENCES

Takeda E, Yamamoto H, Nashiki K, Sato T, Arai H, Taketani Y. Inorganic phosphate homeostasis and the role of dietary phosphorus. J Cell Mol Med. 2004;8(2):191-200.

Sheard PR, Nute GR, Richardson RI, Perry A, Taylor AA. Injection of water and polyphosphate into pork to improve juiciness and tenderness after cooking. Meat Sci. 1999;51(4):371-6.

Calvo MS. Dietary phosphorus, calcium metabolism and bone. The Journal of nutrition. 1993;123(9):1627-33.

Atala A. Re: eIF4E Phosphorylation Promotes Tumorigenesis and is Associated With Prostate Cancer Progression. The Journal of urology. 2011;185(4):1533.

Nikoletopoulou V, Markaki M, Palikaras K, Tavernarakis N. Crosstalk between apoptosis, necrosis and autophagy. Biochimica et biophysica acta. 2013.

Jin H, Xu CX, Lim HT, Park SJ, Shin JY, Chung YS, et al. High dietary inorganic phosphate increases lung tumorigenesis and alters Akt signaling. American journal of respiratory and critical care medicine. 2009;179(1):59-68.

Chang SH, Yu KN, Lee YS, An GH, Beck GR, Jr., Colburn NH, et al. Elevated inorganic phosphate stimulates Akt-ERK1/2-Mnk1 signaling in human lung cells. American journal of respiratory cell and molecular biology. 2006;35(5):528-39.

Reeves PG, Rossow KL, Lindlauf J. Development and Testing of the Ain-93 Purified Diets for Rodents - Results on Growth, Kidney Calcification and Bone Mineralization in Rats and Mice. Journal of Nutrition. 1993;123(11):1923-31.

Hare D, Tolmachev S, James A, Bishop D, Austin C, Fryer F, et al. Elemental bio-imaging of thorium, uranium, and plutonium in tissues from occupationally exposed former nuclear workers. Analytical chemistry. 2010;82(8):3176-82.

Tuquet C, Dupont J, Mesneau A, Roussaux J. Effects of tamoxifen on the electron transport chain of isolated rat liver mitochondria. Cell Biol Toxicol. 2000;16(4):207-19.

Baymann F, van Lis R, ten Brink F, Schoepp-Cothenet B, Nitschke W. Evolution of Rieske/cytochrome b complexes, the enzyme that witnessed the history of life since the Last Universal Common Ancestor. Bba-Bioenergetics. 2012;1817:S90-S.

Nomikos TN, Iatrou C, Demopoulos CA. Application of a TCA-precipitation method for the determination of 1-alkyl-sn-glycero-3-phosphate: Acetyl-CoA acetyltransferase in human renal tissue. Prostaglandins & other lipid mediators. 2004;73(1-2):123-40.

Patsiaoura K, Katsiki E, Tatsiou Z, Hatzitolios A, Alataki D, Douma S. COX-2, BCL-2, tenascin and collagen IV expression in pheochromocytomas. Correlation with malignancy. Histopathology. 2008;53:110-.

Rossi E, Azzone GF. Ion Transport in Liver Mitochondria .4. Relationship between Ion Translocation and Electron Transport. J Biol Chem. 1968;243(7):1514-&.

Kuma A, Matsui M, Mizushima N. LC3, an autophagosome marker, can be incorporated into protein aggregates independent of autophagy: caution in the interpretation of LC3 localization. Autophagy. 2007;3(4):323-8.

Moreno-Torres R, Ruiz-Lopez MD, Artacho R, Oliva P, Baena F, Baro L, et al. Dietary intake of calcium, magnesium and phosphorus in an elderly population using duplicate diet sampling vs food composition tables. The journal of nutrition, health & aging. 2001;5(4):253-5.

Takeda E, Yamamoto H, Yamanaka-Okumura H, Taketani Y. Dietary phosphorus in bone health and quality of life. Nutrition reviews. 2012;70(6):311-21.

Stevens RG, Graubard BI, Micozzi MS, Neriishi K, Blumberg BS. Moderate Elevation of Body Iron Level and Increased Risk of Cancer Occurrence and Death. Int J Cancer.

1994;56(3):364-9.

Durham AC, Walton JM. Calcium ions and the control of proliferation in normal and cancer cells. Bioscience reports. 1982;2(1):15-30.

Untergasser G, Rumpold H, Plas E, Witkowski M, Pfister G, Berger P. High levels of zinc ions induce loss of mitochondrial potential and degradation of antiapoptotic Bcl-2 protein in in vitro cultivated human prostate epithelial cells. Biochem Bioph Res Co. 2000;279(2):607-14.

Fimia GM, Piacentini M. Regulation of autophagy in mammals and its interplay with apoptosis. Cellular and molecular life sciences : CMLS. 2010;67(10):1581-8.

Wei Y, Sinha S, Levine B. Dual role of JNK1-mediated phosphorylation of Bcl-2 in autophagy and apoptosis regulation. Autophagy. 2008;4(7):949-51.

Mamane Y, Petroulakis E, LeBacquer O, Sonenberg N. mTOR, translation initiation and cancer. Oncogene. 2006;25(48):6416-22.

Hsieh AC, Costa M, Zollo O, Davis C, Feldman ME, Testa JR, et al. Genetic dissection of the oncogenic mTOR pathway reveals druggable addiction to translational control via 4EBP-eIF4E. Cancer cell. 2010;17(3):249-61.

Flynn A, Vries RG, Proud CG. Signalling pathways which regulate eIF4E. Biochemical Society transactions. 1997;25(2):192S.

Fujimura K, Sasaki AT, Anderson P. Selenite targets eIF4E-binding protein-1 to inhibit translation initiation and induce the assembly of non-canonical stress granules. Nucleic Acids Res. 2012;40(16):8099-110.

Yang SX, Hewitt SM, Steinberg SM, Liewehr DJ, Swain SM. Expression levels of eIF4E, VEGF, and cyclin D1, and correlation of eIF4E with VEGF and cyclin D1 in multi-tumor tissue microarray. Oncology reports. 2007;17(2):281-7.

Ducker GS, Atreya CE, Simko JP, Hom YK, Matli MR, Benes CH, et al. Incomplete inhibition of phosphorylation of 4E-BP1 as a mechanism of primary resistance to ATP-competitive mTOR inhibitors. Oncogene. 2013.

국문 논문 초록

고농도 무기인산염의 섭취가 초기 폐암진행에 미치는 영향

(지도 교수: 조 명 행)

이 소 민

서울대학교 대학원

의과대학 종양생물학협동과정

무기인산(Pi)은 특정 유전자나 신호전달체제를 조절하며 뼈나 근육 뇌 또는 폐와 같은 조직의 성장에 영향을 주기 때문에 살아있는 생명체에게 없어서는 안될 꼭 필요한 물질이다. 본 연구의 목적은 고농도 무기인산 섭취 시 무기인산과 관련된 신호들을 in vivo에서 관찰 하는 것 이다. 실험에 사용된 K-ras^{LA1}은 폐암 모델 마우스이다. K-ras^{LA1} 개체들은 임의로 두 분류로 나뉘어져 한 그룹은 0.3% 무기인산이 함유된 normal diet (ND)를, 다른 한 그룹은 1%의 무기인산이 함유된 high phosphate diet (HPD)를 1, 2, 4개월동안 진행 하였다. 실험 진행 후, 모든 샘플들은 ICP-MS/OES, LA-ICP-MS analyses, Western blot, histopathological examination, immunohistochemistry (IHC), and immunofluorescence (IF) labeling을 하는데 사용 되었다. 실험결과는 고농도 무기인산 섭취가 암 발생을 가속화시키고 종양의 크기도 증가시켰다. 하지만, 4개월동안 고농도 무기인산 섭취를 한 군에서는 제한된 종양성장을 보여주었고 간과 폐에서 이온들의 증감이 현격히 관찰 되었으며, 모든 HPD군에서 TCA 회로를 통한 에너지 생산과 활발한 세포자식증의 관찰, 신 혈관 생성의 감소, 단백질 번역 양과 세포자살의 증가를 보였다. 이러한 결과들을 토대로 고농도 무기인산의 섭취가 초기의 폐암 성장을 증가시키고 장기 섭취 시에도 metabolic adaptation을 통하여 암 화가 계속된다는 결론을 얻을

수 있었다. 따라서 적당량의 무기인산섭취가 폐암의 예방 및 치료에 중요한 역할을 한다는 것이 본 연구를 통해 입증되었다.

주요어: 고농도 무기인산 섭취, 무기인산, 폐암, 세포자식증, 단백질번역, 세포자살, 종양생장

학번 : 2012-21771